ELSEVIER

Polymer 43 (2002) 7161–7170

polymer

www.elsevier.com/locate/polymer

Surface properties of fluorinated oxetane polyol modified polyurethane block copolymers

Yu-Seung Kim, Jae-Suk Lee[1], Qing Ji[2], James E. McGrath*

Department of Chemistry and Materials Research Institute, Virginia Polytechnic Institute and State University, 107 Davidson Hall, Blacksburg, VA 24061-0344, USA

Received 9 August 2001; received in revised form 22 February 2002; accepted 21 May 2002

Abstract

This article describes the surface properties of fluorinated oxetane polyol (F-Polyol) containing linear segmented polyurethane elastomers. A series of polyurethane elastomers derived from a soft segment based on 2300 g/mol polyhexamethylene carbonate, and a hard segment composed of 4,4′-methylene diphenyl diisocyanate chain extended with 1,4-butanediol were modified with a 3285 g/mol F-Polyol via either melt or solution reaction in dimethyl acetamide. X-ray photoelectron spectroscopy confirmed that the surfaces of the modified polyurethanes exhibit notable fluorine enrichment within the uppermost 5 nm, depending on the bulk composition and the polymerization method. Field emission scanning electron microscopy and tapping mode atomic force microscopy experiments demonstrated that relatively large micro-scale domain structures were exclusively found in the melt-polymerized polyurethanes. This was attributed to incompatibility of the F-Polyol with the other reactive constituents during the melt polymerization. Friction experiments revealed that the friction coefficient of the fluorinated polyurethanes decreased by about 2-fold as the surface fluorine concentration increased from 0 to about 20 at.%. Furthermore, the melt-polymerized polyurethanes underwent a stick-slip motion, whereas the more homogeneous solution-polymerized polyurethanes experienced a conventional stable sliding. These friction behaviors are discussed in terms of the surface topography and morphology.

Keywords: Segmented polyurethane elastomer; Fluoro-oxetane polyol; Fluorine

1. Introduction

Fluorinated polymers have been widely used in hydrophobic coatings and medical devices because of their excellent environmental stability, water and oil repellency, and low coefficient of friction [1,2]. Incorporation of fluorine into the polymer main chain or side chain is well known to lead to large changes of the surface properties as the fluorinated polymer chains segregates toward the polymer–air interface, resulting in considerable decrease in the surface energy [3–8]. Segmented polyurethane elastomers are one material that would benefit from the characteristic properties of fluorinated polymers, as mentioned above [1,9–12].

In general, polyurethane elastomers have a complex micro-phase separation primarily due to the incompatibility of the soft, and hard segments. Phase separation and morphology studies of segmented polyurethane elastomers have been based mostly on small angle X-ray scattering and electron microscopy; these techniques showed that phase separated domain structures resulting from the incompatibility of soft segments alternating with stiff segments originating from isocyanate groups in a block copolymer appeared in a size of several nanometers [13–16].

Fluorinated polyurethanes, however, may have more complex surface structures because of the surface segregation of the fluorinated polymer chain. Consequently, the surface structures of fluorinated polyurethanes are strongly dependent on not only the molecular structure of each segment, and their composition, but also the polymerization method since melt polymerization utilizing the fluorinated chain segments produces systems that are incompatible with the other segments, while solution methods can produce homogeneous mixing during the polymerization [17–19].

* Corresponding author. Tel.: +1-540-231-4457; fax: +1-540-231-8517.
E-mail address: jmcgrath@vt.edu (J.E. McGrath).
[1] Present address: Department of Materials Science and Engineering, Kwangju Institute of Science and Technology, Kwangju 500-712, South Korea.
[2] Present address: Dexter Corporation, Los Angeles, CA, 91746, USA.

0032-3861/02/$ - see front matter
PII: S0032-3861(02)00458-5

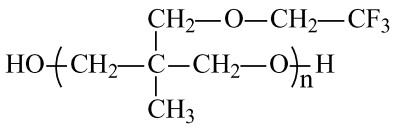

Fig. 1. Chemical structure of a fluorinated oxetane polyol (F-Polyol).

Several articles have reported the surface structures of the modified polyurethane elastomers with respect to their chemistry, surface energy, morphology and micro-heterogeneity [11,16–21]. However, they are limited in their ability to provide the influence of polymerization method upon the surface structure. Besides, there are surprisingly few studies in the scientific literature concerned with friction behavior of surface modified polyurethanes [22,23].

Our aim in this study was to investigate the surface properties including surface composition, surface morphology and friction behavior, of the polyurethane elastomers with a novel fluorinated oxetane polyol (F-Polyol) [24] (Fig. 1), primarily in terms of polymerization method and fluorine content. The incorporation of the F-Polyol into polyurethane elastomers was conducted based on 4,4′-diphenylmethane diisocyanate (MDI) chain extended with 1,4-butanediol (BD) by the partial replacement of polyhexamethylene carbonate (PHMC) polyol soft segment at a fixed soft segment concentration of 62 wt%. A series of F-Polyol containing polyurethane samples were produced via either melt or solution polymerizations. The surface compositions of the polyurethane films cast from dimethyl acetamide (DMAc) were analyzed by X-ray photoelectron microscopy (XPS). Surface morphology of the polyurethane films was observed using field emission scanning electron microscopy (FE-SEM) and tapping mode atomic force microscopy (AFM). Friction behavior was investigated in a plate-on-plate geometry in contact with a cleaned aluminum counter surface. The friction behavior, including stick-slip and smooth sliding motions are explained by a proposed model, that is based on morphological evidence.

2. Experimental

2.1. Materials

Primary hydroxyl terminated PHMC, ($M_n = 2300$, Bayer, Inc.), MDI (Bayer) and 1,4-butanediol (BD) (Aldrich) were used as received without further purification. DMAc and toluene were dried over calcium hydride and then fractionally distilled under vacuum. Fluorinated oxetane polyol (F-Polyol, $T_g = -49$ °C, Omnova Solutions, Inc.) was purified by vacuum stripping at about 160 °C to remove cyclic fractions. The proton NMR spectrum (Fig. 2) for purified F-Polyol showed that the F-Polyol contained 2.8 wt% of tetramethylene oxide sequences, which was efficiently incorporated randomly in the copolymer. The number average molecular weight (M_n) of F-Polyol was

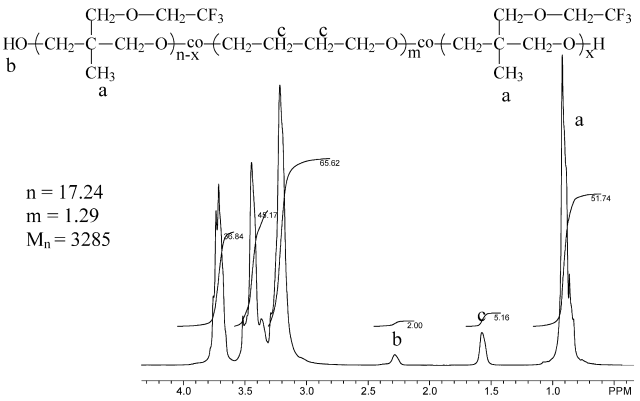

Fig. 2. Proton NMR spectra of purified F-Polyol.

3285 g/mol calculated from the NMR end group analysis. The molecular structure of the F-Polyol was also characterized by gel permeation chromatography, liquid chromatography, and gas chromatography-mass spectroscopy [25].

2.2. Synthesis and film casting

Fluorinated polyurethane elastomers were synthesized via either melt or solution polymerization. The fluorine concentration in the polyurethane was controlled by the ratio of F-Polyol to PHMC polyol, which were used as co-soft segments.

For melt polymerization, PHMC polyol, MDI and F-Polyol were separately weighed and heated to 100 °C. The F-Polyol was added into the MDI, stirred and heated at 100 °C for 30 min. After mixing, the reaction system was still homogeneous. The PHMC polyol was then added, stirred and heated at 100 °C for another 30 min. Once the PHMC polyol was added, the reaction system became cloudy, which suggests F-Polyol immiscibility with PHMC polyol. BD chain extender was added and stirred for 10 min at 100 °C, then poured into a mold. The polymer was post-reacted at 100 °C in an air circulation oven for 15 h.

For solution polymerization, DMAc was employed to develop a series of polyurethane elastomers. PHMC, F-Polyol and BD chain extender were dissolved in DMAc/toluene and charged into a flask. The reaction system was heated to 100–130 °C and maintained at that temperature for 2 h. It was then dehydrated through azeotropic distillation of toluene before addition of the MDI. After 2 h, all toluene was removed. After cooling the solution to 60 °C MDI and 0.5 wt% dibutyltin dilaurate catalyst were added. The reaction temperature was raised to 100 °C for 2 h, which afforded very viscous solutions.

All solid films were prepared by solution casting. The polyurethanes were dissolved in DMAc (20% w/v) and cast onto glass plates, which were preheated to 80 °C. Cast films were kept at 50 °C in an air circulation oven for 24 h and subsequently at 100 °C in a vacuum oven for 24 h. The films were stored at room temperature at least two weeks before any testing. One should note that the fluorinated

Table 1
Reaction formulation of F-Polyol containing segmented polyurethane elastomers

Sample[a]	Molar ratios				F-Polyol (wt%)
	MDI	PHMC	F-Polyol	BD	
PUC-X-00	4	1	0	3	0
PUC-X-0.1	4	0.999	0.001	3	0.1
PUC-X-0.5	4	0.995	0.005	3	0.5
PUC-X-1.0	4	0.99	0.01	3	1.0
PUC-X-9.2	4.2	0.9	0.1	3.2	9.2
PUC-X-38.2	5	0.5	0.5	4	38.2

[a] X refers to reaction type, i.e X = S when via solution reaction, X = M when via melt reaction.

polyurethane films prepared via melt reactions were opaque while the films via solution reaction were colorless and transparent. All fluorinated polyurethanes were thermally stable up to 250 °C in air based on the previous TGA data [19].

The sample code used in this paper is based on the reaction type and F-Polyol content. For example, PUC-S(or M)-1.0 refers to a polyurethane via solution reaction (or melt reaction) containing 1.0 wt% of F-Polyol. All samples contained 62 wt% of soft segment.

Table 1 summarizes the molar ratios and weight fractions of F-Polyol containing polyurethane copolymers for the reactions.

2.3. Measurements

Gel permeation chromatography (GPC). The molecular weight and distribution of the polymers was analyzed by GPC on a Waters 2690 separations module equipped with a differential refractometer detector and an on-line differential viscometer detector (Viscotek T60A) coupled in parallel. Waters μ styragel HR0.5 + HR2 + HR3 + HR4 column bank were used. *N*-methylpyrrolidone (HPLC grade) containing 0.02 M P_2O_5 served as a mobile phase. The flow rate was 1.0 ml/min, the injection volume was 100 μl, and the column temperature was 60 °C. TriSEC GPC software V3.0 (ViscoTek) was used to acquire and analyze the data. A series of narrow molecular weight distribution polystyrene standards (Polymer Laboratory) was employed to generate the universal calibration curve.

X-ray photoelectron spectroscopy (XPS). Surface compositions were analyzed on an angle-dependent XPS (Perkin–Elmer physical electronic model 5400) with a hemispherical analyzer and a position sensitive detector. The spectrometer was equipped with a Mg Kα achromatic X-ray source (300 W, 14 kV) and two take off angles (TOAs) of 15° and 90° were used with the X-ray source. The spot size used was 1×3 mm^2. Survey scans were taken in the range of 0–1100 eV. Any significant peaks in the survey scan were then subjected to narrow scans in the appropriate ranges for atomic concentration analysis. The binding energy of each photopeak was referenced to C_{1s} level from ubiquitous organic material at 285.0 eV. A pass energy of 44.75 eV was chosen for all angle-dependent acquisitions. The spectrometer was typically run at the 10^{-8} Torr vacuum range.

Microscopy. FE-SEM and tapping mode AFM were used to obtain surface morphology and topography. FE-SEM (Leo 1550 Gemini) was operated at a low incident beam voltage (7 kV) to minimize charging. Secondary electron signals were collected from an in-lens detector. The energy dispersive X-ray analysis (EDX) of the surface was also done on the attachment to the FE-SEM. Prior to analysis, the air-contacting surfaces of the samples were sputter coated with an about 2 nm layer of gold.

Height and phase images were recorded simultaneously on an AFM (Dimension 3000, Digital Instruments) operated at room temperature, using the micro-fabricated cantilevers with force constant of approximately 40 N/m. For image analysis, the Dimension 3000 image processing software was used. In tapping mode, the level of force applied to the surface can dramatically change the data [26]. For this study, the ratio of amplitudes which are used in feedback control was adjusted to 0.57 of the free air amplitude for all the reported images. Under this moderate force tapping conditions, phase data are sensitive to local stiffness differences of domains in the top several nanometers from the uppermost surface.

Mechanical properties. Tensile properties were measured on an Instron tensile testing machine (model 4204) using cross-head at a speed of 25.4 mm/min. Dumbbell shaped tensile specimens (Type V) were used according to ASTM 638-94.

Friction behavior. The setup for observing friction behavior was based on the ASTM D1894 guide. The rectangular aluminum sled (200 g, $63.5 \times 63.5 \times 15$ mm^3) was machined for the test. After a nylon string was attached to the sled, it was pulled 20 mm at 150 mm/min with a tensile tester (Instron model 4204) at ambient conditions. The friction force was recorded as a function of the displacement of the sled. Static and kinetic friction coefficients were calculated. Before each test, the counter aluminum surface of the sled was cleaned with acetone to remove all contaminants. At least three individual measurements were conducted at each given sample.

3. Results and discussion

3.1. GPC Analysis

The structure of the fluorinated polyurethane elastomers depends strongly on the polymerization method as well as on the reaction conditions and the reactivity of components. For this study, the fluorinated polyurethane elastomers were prepared by two different polymerization methods, i.e. via melt reaction or via solution reaction. Fig. 3 shows the GPC

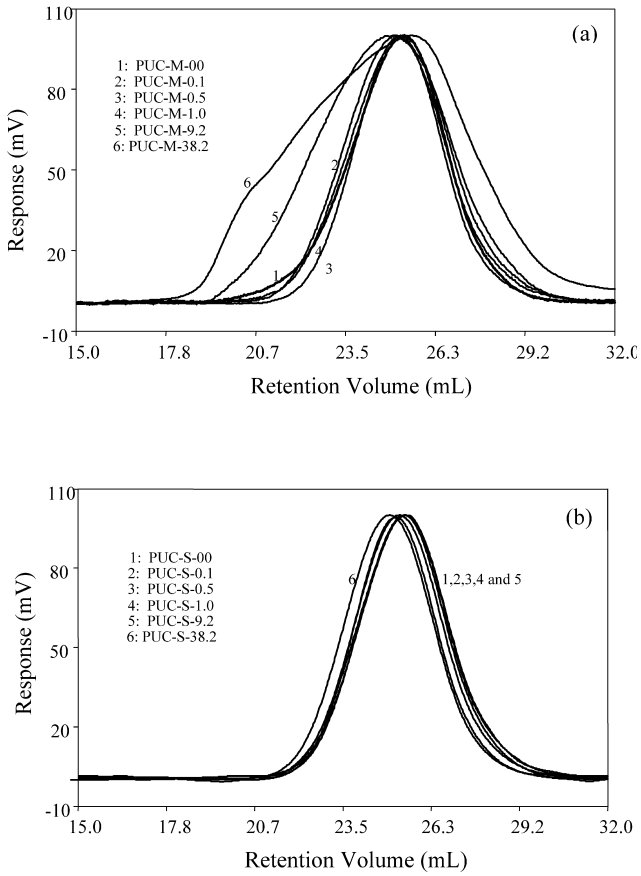

Fig. 3. Gel permeation chromatograms of F-Polyol containing polyurethane elastomers made from (a) melt polymerization and (b) solution polymerization.

traces of the fluorinated polyurethane elastomers in terms of polymerization methods. The absence of low molecular weight peak or shoulder at around 27 mL retention volume indicated that all fluorinated polyurethanes did not contain unreacted polyols [25]. The GPC traces showed that the melt-polymerized polyurethane elastomers had a broader molecular weight distribution while the polyurethanes via solution reaction had a narrower and unimodal distribution.

Table 2
Molecular weight and molecular weight distribution of F-Polyol containing segmented polyurethane elastomers from GPC

Sample code	M_n	M_w	M_w/M_n
PUC-M-00	21,500	40,500	1.9
PUC-M-0.1	18,600	34,600	1.9
PUC-M-0.5	20,500	39,100	1.9
PUC-M-1.0	18,000	35,600	2.0
PUC-M-9.2	14,400	34,500	2.4
PUC-M-38.2	10,600	38,200	3.6
PUC-S-00	22,300	42,200	1.9
PUC-S-0.1	18,500	33,300	1.8
PUC-S-0.5	20,200	38,800	1.9
PUC-S-1.0	21,200	41,300	1.9
PUC-S-9.2	23,600	43,400	1.8
PUC-S-38.2	27,800	53,200	1.9

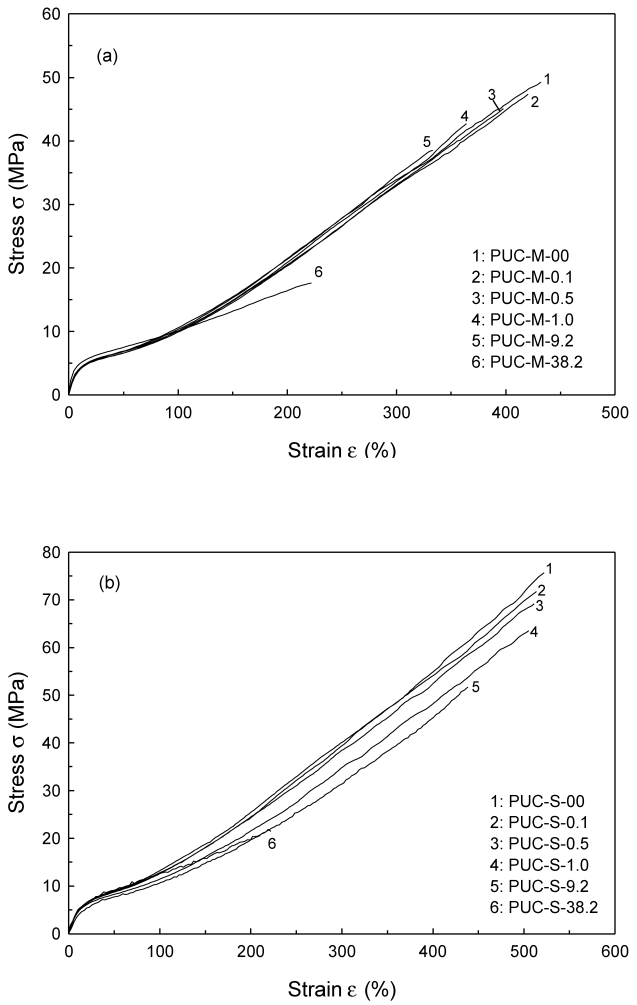

Fig. 4. Stress–strain curves of F-Polyol containing polyurethane elastomers made from (a) melt polymerization and (b) solution polymerization.

In particular, the broadness of the melt-polymerized polyurethanes became more significant at higher F-Polyol concentration. These were a result of the limited compatibility between the F-Polyol and PHMC-polyol. In contrast, the solution-polymerized polyurethanes always produced transparent and clear films, indicating that the solution polymerization proceeded homogeneously in DMAc. Table 2 summarizes the molecular weights and molecular weight distributions of the F-Polyol containing polyurethane elastomers.

3.2. Mechanical properties

Stress–strain curves of the fluorinated polyurethane elastomers are shown in Fig. 4. All samples except PUC-S or M-38.2 exhibited soft segment crystallization under strain due to PHMC soft segments (opaque on stretching). The result shows that all these samples have high tensile strength at break except PUC-S or M-38.2. The elongation at break decreases with increasing fluorine content. Compared with the samples made from melt polymerization, the

Table 3
Fluorine atomic compositions of the surface of F-Polyol containing segmented polyurethane elastomers

Sample	F_{1s} at.%			Fluorine surface enrichment factor[b]
	15° TOA	90° TOA	Cal.[a]	
PUC-M-00	0.4	0.2	0	–
PUC-M-0.1	6.5	3.8	0.02	190
PUC-M-0.5	16.7	11.0	0.1	110
PUC-M-1.0	18.9	15.2	0.2	76
PUC-M-9.2	19.1	17.6	2.1	8
PUC-M-38.2	19.4	19.2	8.7	2
PUC-S-00	0.2	0.1	0	–
PUC-S-0.1	12.7	9.2	0.02	460
PUC-S-0.5	19.2	16.4	0.1	164
PUC-S-1.0	19.1	17.2	0.2	86
PUC-S-9.2	19.9	18.3	2.1	9
PUC-S-38.2	20.4	19.4	8.7	2

[a] Calculated by the bulk content from the chemical structures of the polymers.
[b] (Measured atomic% of fluorine at 10° TOA)/(calculated atomic% of fluorine).

polyurethane made from solution polymerization exhibited better tensile properties.

3.3. Surface compositions

It is well known that the low surface free energy of the component provides a thermodynamic driving force for migration to the polymer–air interface. XPS studies conducted on the low surface energy materials such as polydimethylsiloxane containing copolymers showed that surface segregation occurred even when the amount of low surface energy material incorporated during the synthesis was relatively small [17]. For this study, angle-dependent XPS was used to quantify the surface composition of the fluorinated polyurethane elastomers. The sampling depth was varied by collecting data at take-off angle (TOA) between the sample surface and the analyzer of 90° and 15°.

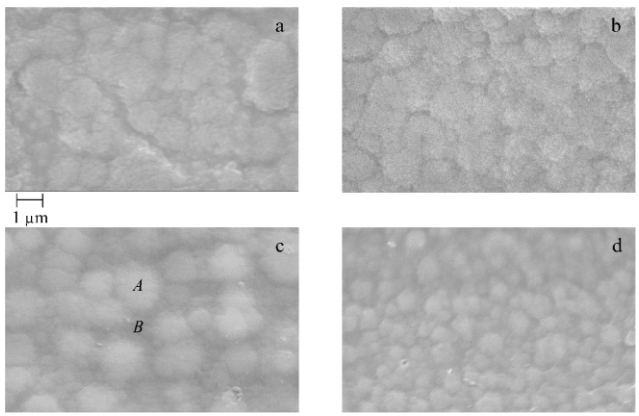

Fig. 5. Surface morphology of the melt-polymerized F-Polyol containing polyurethane elastomers: (a) PUC-M-00, (b) PUC-M-0.1, (c) PUC-M-1.0, (d) PUC-M-38.2. EDX analysis shows the ratios of fluorine to oxygen of the region A and region B shown in (c) are 0.46 and 1.39, respectively.

The 90° TOA corresponds to an integrated depth sensitivity of about 5 nm and for the TOA of 15°, the detection depth is around 1 nm.

Table 3 displays the surface fluorine atomic percentage of the F-Polyol containing polyurethane elastomers. Disregarding unavoidable fluorine contamination at levels about 0.2%, the fluorine concentrations on the surface for F-Polyol containing samples were much higher than calculated bulk concentrations, which implied that the surface was enriched with fluorine segments. The fluorine concentration in the uppermost surface dramatically increase up to about 19 at.% and tended to level off at around 1 wt% of F-Polyol. Considering that the calculated fluorine at% of F-Polyol is about 24.1, this result suggests that most of the fluorinated soft segment is present in the uppermost 5 nm of the polymer surface. The observation of a surface enrichment of the fluorine segments are in quantitative agreement with prior observations in the investigation of poly(tetramethylene oxide) based F-Polyol containing polyurethane elastomers [18–20].

In addition, the results showed that the surface enrichment of fluorine of the polyurethane with lower F-Polyol content (less than 9.2 wt%) was more significant than for that with higher F-Polyol content as seen in the dramatic reduction of the fluorine surface enrichment factor with F-Polyol content. In other words, the high fluorine content polyurethanes had less of an influence on the surface enrichment throughout the sampling depth profile. This suggests that a thicker fluorine-rich surface layer might have formed on the polyurethanes with higher F-Polyol content.

The polyurethane synthesized in solution showed, in general, higher fluorine surface enrichment than for those via melt polymerization and this phenomenon was more significant at 90° TOA. For example, when the F-Polyol composition is 0.5 wt%, the fluorine surface enrichment factor for the solution-polymerized sample is 164, approximately 1.5 times higher than that of melt-polymerized sample.

3.4. Surface morphology

The influence of polymerization method upon the surface morphology of F-Polyol containing polyurethane elastomers can be readily observed using FE-SEM. Fig. 5 compares the surface morphology of the polyurethane elastomers prepared via melt-polymerization. The micrographs of all melt-polymerized polyurethanes including the PUC-M-00 control sample displayed a relatively large phase separated domain structure: the discontinuous bright domains appeared in the dark continuous phase. The phase separation of the PUC-M-00 control sample is presumably due to the local surface contamination of fluorine. Upon decreasing F-Polyol concentration, the domain size of the bright discontinuous domains decreased and the shape of the domains tended to be regular and spherical. These bright domains were assigned to the PHMC-rich domains and the

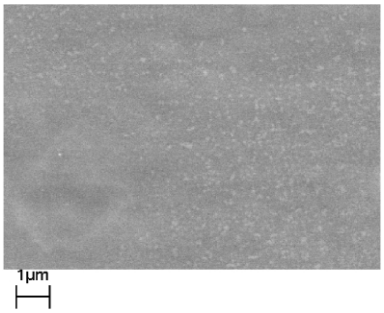

Fig. 6. Surface morphology of the solution polymerized F-Polyol containing polyurethane elastomer, PUC-S-1.0.

dark continuous phase was fluorine-rich phase by using EDX measurement, which showed the fluorine content of the dark phase is much higher than that of the bright phase. For example, the bright phase marked A in Fig. 5(c) had a fluorine to oxygen atomic ratio of 0.46 while the ratio of the dark phase marked B in Fig. 5(c) was 1.39.

Comparatively, the solution-polymerized polyurethane elastomers did not exhibit the macro-scale phase separation as appeared in the melt-polymerized polyurethanes. Fig. 6 shows the representative surface morphology of the solution-polymerized polyurethanes. In spite of the fact that the surface of the solution-polymerized polyurethane seemed to be more or less wavy, no macro phase separation was observed.

These FE-SEM data demonstrate that the melt-polymerized polyurethanes had a heterogeneous domain structure in which fluorinated segments were unevenly distributed, while in the case of the solution-polymerized polyurethanes, fluorinated segments might be distributed uniformly over all surfaces of the samples. The existence of the fluorine-poor phase, that is PHMC-rich phase, found in the melt-polymerized polyurethanes probably causes a relatively low surface concentration of fluorine compared to the solution-polymerized polyurethanes because the area fraction of the surface covered by fluorine was less. This result was consistent with the XPS data that showed lower fluorine enrichment of melt-polymerized samples. Furthermore, the macro-scale phase separation explains the opacity of the melt-polymerized polyurethanes, which is generally considered to be indicative of a phase-separated morphology and is attributed to the scattering of light from the immiscible domains having distinctly different refractive indices.

The AFM technique was used to further understand the surface morphology. For scanning probe studies of polymers, in general, the phase and height images are dramatically affected by the tip-sample force interaction, which can be adjusted by the ratio of the engaged amplitude to the free air amplitude [5,12,23,29]. That is to say, the ratio of amplitude in the range of 0.75–0.9, i.e. light force tapping resolves about 0–5 nm below the surface whereas the ratio of amplitudes with a range of 0.4–0.7, i.e. moderate force tapping, resolves domains lying underneath

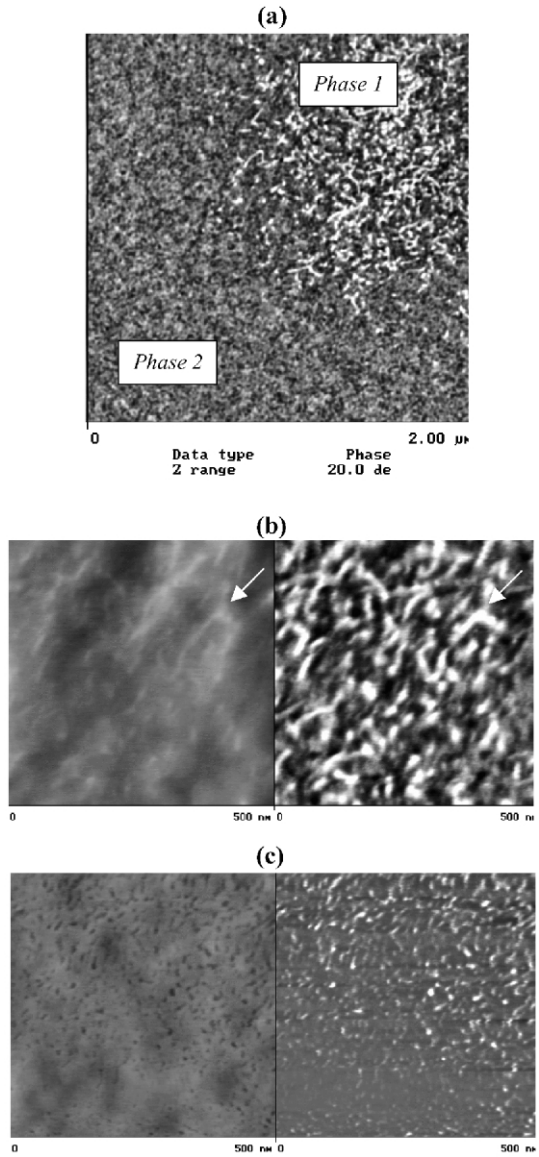

Fig. 7. AFM tapping mode images of the melt-polymerized F-Polyol containing polyurethane elastomer, PUC-M-1.0. (a) Phase image of 2 × 2 μm with phase scale of 0–20°. No height image is shown. (b) Height image (left) and phase image (right) of Phase 1. Scan area is 500 × 500 nm and the height scale and phase scale are 0–10 nm and 0–20°, respectively. Arrows indicate representative hard segment rich phase. (c) Height image (left) and phase image (right) of Phase 2. Scan area is 500 × 500 nm and the height scale and phase scale are 0–10 nm and 0–20°, respectively.

the uppermost surface layer. In our experiments, when we applied a high ratio of amplitude (about 0.8) on melt-polymerized polyurethanes, the phase image was essentially featureless, indicating the uppermost surface was probably homogeneous without any distinct phase separation. However, as the ratio of amplitude is decreased down to 0.57, phase-separated domain structure on the near surface region was clearly exhibited.

Fig. 7 shows the near surface structure of PUC-M-1.0 sample by moderate force tapping mode AFM. The phase

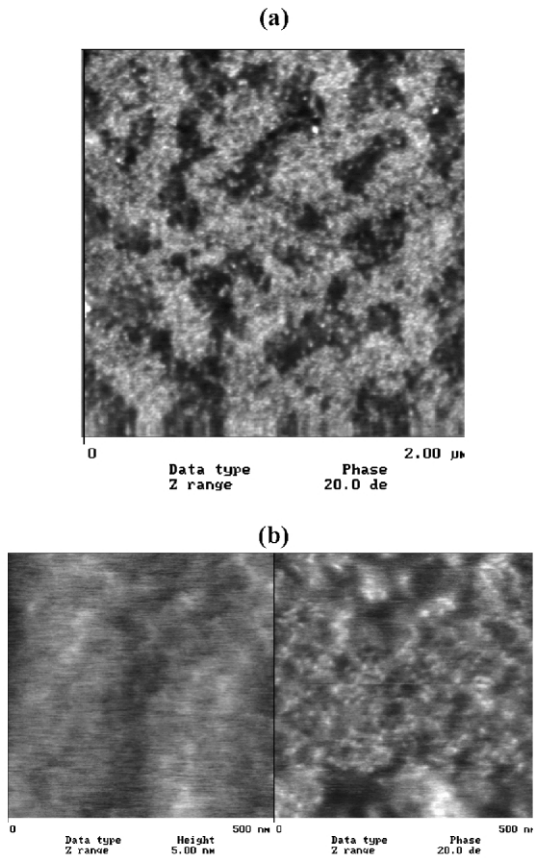

Fig. 8. AFM tapping mode images of the melt-polymerized F-Polyol containing polyurethane elastomer, PUC-S-1.0. (a) Phase image of 2×2 μm with phase scale of 0–20°. No height image is shown. (b) Height image (left) and phase image (right) of Phase 1. Scan area is 500×500 nm and the height scale and phase scale are 0–5 nm and 0–20°, respectively.

contrast image shows a relatively large-scale phase separation, of which domain size is similar to the micrograph observed by FE-SEM. The surface morphology clearly shows that one phase, which is referred to as Phase 1, gains more phase contrast than the other phase, Phase 2. A higher resolution, 500 nm height and phase image pairs are shown in Fig. 7(b) and (c). Although the phase images exhibited a higher contrast than do height images, for Phase 1, the bright phase is placed in higher than the dark phase, which is easily recognized by comparing the contrast of marking arrows in the identical point. However, Phase 2 shows that the bright spots in the phase image appeared as dark spots in the height image, which means, the bright hard segments exist in height lower than the soft segments as shown in Fig. 7(d) In these AFM data, it is clear that the bright region corresponds to the hard segment-rich phase and the dark region belongs to soft segment-rich phase since the region having higher modulus appeared to be brighter in the AFM operating conditions. The direct assignment of the micro-phase domains from the stiffness of fluorinated segments is not possible since the stiffness of fluorinated segments strongly depends upon the molecular structure of the segments [6,27]. However, considering Phase 1 is a discontinuous phase, which turned out to be a PHMC-rich phase by FE-SEM, and the surface morphology of Phase 1 has been found in most segmented polyurethane elastomers [15,28], it is not unreasonable that the Phase 2 is developed by introducing the fluorinated segments. Thus, one can conclude that the MDI hard segments were located on the uppermost surface in the PHMC-rich phase but at a lower height in the F-Polyol-rich phase because the fluorinated segments have the high affinity to the air interface.

The solution-polymerized polyurethane exhibited an interesting morphology by moderate force mode AFM. Fig. 8 shows the phase image of a representative specimen. Although the phase contrast was not as pronounced as that of the melt-polymerized samples, worm-like co-continuous domains with widths in the 0.2–0.3 μm range were found. These domain structures are qualitatively similar to the micro phase separation expected for segmented copolymers, [29] in spite of the fact that this surface structure was not observed in the micrographs by FE-SEM. This could presumably be due to the low phase contrast of the electron microscopy. Since the hard segment-rich area is the bright spot and the soft segment-rich area shows up as a dark spot, phase segregation is apparently driven by the thermodynamic incompatibility between the hard segments and the soft segments. The local height difference between those two phases was small making it impossible to assign by a stiffness difference as shown in Fig. 8(b). This result indicated that the fluorinated segments of the solution-polymerized polyurethanes are uniformly distributed within both segment-rich phases and contributes to a decrease of the height difference between the phases.

3.5. Friction behavior

Fig. 9 shows the friction forces curves recorded for the fluorinated polyurethanes as a function of displacement. As we show, all melt-polymerized polyurethanes undergo a periodic stick-slip motion while the solution-polymerized polyurethanes show a stable sliding motion. We will discuss the mechanism of the stick-slip motion in later section.

The influence of the fluorine content upon the friction coefficient were examined by determining the friction coefficient for both systems. The kinetic friction coefficient, F_k, for the stick-slip motion was calculated, assuming it to be single valued, is half value between the top and the bottom of the slip [30]. In other words, we used following equations to calculate the friction coefficient of the stick-slip motion:

$$F_s = F_t \tag{1}$$

$$F_k \approx (F_t + F_b)/2; \tag{2}$$

where F_s and F_k are true static and kinetic friction forces, respectively, F_t and F_b are the top and the bottom friction forces, respectively.

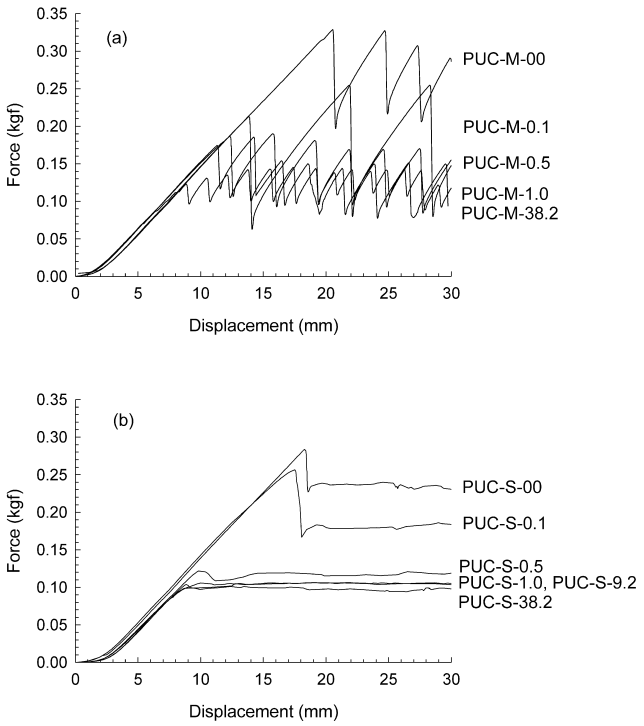

Fig. 9. Force–displacement curves of the F-Polyol containing polyurethane elastomers made from (a) melt polymerization (b) solution polymerization.

Table 4 summarizes the friction coefficients of fluorinated polyurethanes. Regardless of the polymerization method, the friction coefficients of the fluorinated polyurethanes significantly decreased with F-Polyol concentration. Control polyurethane elastomers showed the highest values both of static and kinetic friction coefficients, while the polyurethanes containing 38.2 wt% of F-Polyol exhibited the lowest values, that were approximately 2-fold lower than those of the unmodified polyurethanes. Furthermore, it is worthy to note that low friction can be achieved even at very low F-Polyol concentration, which suggests the friction coefficient can be directly correlated with the surface

Table 4
Friction coefficient of the F-Polyol containing segmented polyurethane elastomers

Sample	Friction coefficient	
	Static	Kinetic
PUC-M-00	1.59 ± 0.04	1.32 ± 0.04
PUC-M-0.1	1.22 ± 0.09	1.00 ± 0.06
PUC-M-0.5	0.89 ± 0.04	0.68 ± 0.03
PUC-M-1.0	0.79 ± 0.08	0.62 ± 0.08
PUC-M-9.2	0.80 ± 0.05	0.60 ± 0.04
PUC-M-38.2	0.69 ± 0.04	0.59 ± 0.02
PUC-S-00	1.42 ± 0.11	1.16 ± 0.04
PUC-S-0.1	1.04 ± 0.10	0.76 ± 0.06
PUC-S-0.5	0.65 ± 0.04	0.60 ± 0.03
PUC-S-1.0	0.56 ± 0.06	
PUC-S-9.2	0.52 ± 0.02	
PUC-S-38.2	0.49 ± 0.01	

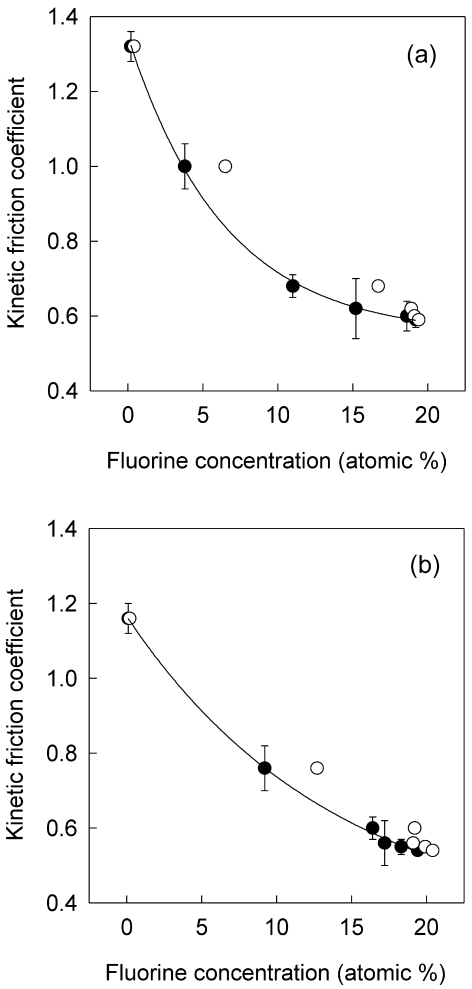

Fig. 10. Dependence of the surface fluorine content upon kinetic friction coefficients. (a) Melt-polymerized polyurethane elastomer. (b) Solution-polymerized polyurethane elastomer: ●, 90° TOA; ○, 15° TOA.

fluorine content. The dependence of the surface fluorine concentration upon the friction coefficient is displayed in Fig. 10; the kinetic friction coefficient versus the surface fluorine atomic% was obtained from XPS results. As expected, the plot shows that the friction coefficient was inversely proportional to the surface fluorine concentration of both systems. In particular, it was found that the correlation with the surface fluorine concentration at 90° TOA is more plausible than with the fluorine concentration at 15° TOA, indicating that the friction reduction depends more upon the near surface structure. Similar effects related to the layer thickness dependence on friction force were found in dimethylsiloxane-*b*-styrene copolymers [31]. With respect to the reaction type, it appears that solution-polymerized polyurethanes lowered the friction coefficient more than melt-polymerized polyurethanes in both static and kinetic friction coefficients.

A distinct characteristic of the friction behavior found in melt-polymerized polyurethanes is stick-slip motion as shown in Fig. 9. It is well known that the testing conditions are critical to generate stick-slip motion [32–33]. However,

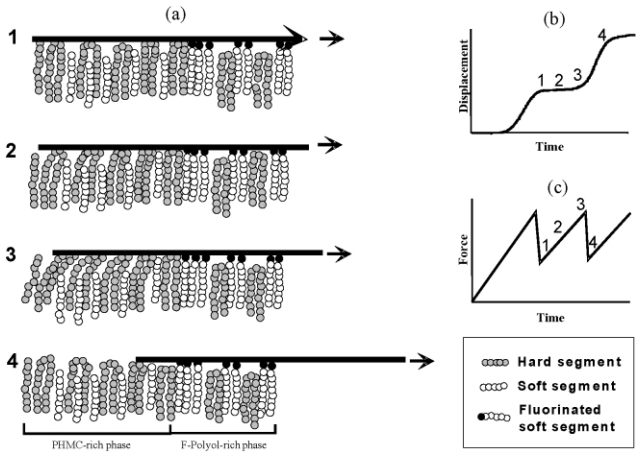

Fig. 11. Proposed model of the stick-slip motion for the melt-polymerized F-Polyol containing polyurethane elastomers. This figure shows that PHMC-rich phase adhere to the counter surface during shear sliding, i.e. steps 1–3, to decelerate displacement and increase friction force and when the friction force overcome the adhesive strength, counter surface released at a moment, i.e. step 4, to rapid increase displacement and sudden drop of friction force. (a) Schematic illustration of the stick-slip motion on the surface. (b) Displacement change with time at interface. (c) Friction force change with time.

we found that the stick-slip motion depicted in Fig. 8 may be considered as characteristic of the surface structure, more precisely the near surface structure, since all other factors such as normal pressure and sliding velocity are the same.

The origin of stick-slip motions has been extensively reviewed by Israelachvili et al. [33,34]. According to them, stick-slip motion occurring during solid-on-solid sliding can be generated by two different mechanism; (1) surface roughness model in which protruding asperities are bumped together during sliding or (2) creep model in which a characteristic distance has to be moved to break adhesive junctions.

Those models enable us hypothesize that the origin of stick-slip motion found the polyurethane samples can be caused either by surface corrugations or by, so called, adhering asperity junctions. Obviously, the stick-slip motion found in the melt-polymerized polyurethanes, however, could not fall into the surface roughness model since AFM height image showed no significant roughness difference between the melt-polymerized and the solution-polymerized polyurethanes (e.g. root mean square (RMS) surface roughness for PUC-M-1.0: 0.45 nm; RMS roughness for PUC-S-1.0: 0.60 nm). On the other hand, the creep model can explain the stick-slip behavior of the melt-polymerized polyurethanes as shown in Fig. 11. That is to say, the PHMC-rich phases have the role of adhesive junctions having a characteristic length. During shear sliding, the friction force builds up with time until the friction force overcomes the adhesion force between the PHMC rich-phase and the counter surface (steps 1–3 in Fig. 11). During this stage, displacement of the contacting surface is fixed with time (see curves for displacement vs. time in Fig. 11). Once the adhesion force is overcome, the friction force decreases rapidly and reached a minimum value and the displacement abruptly increased (step 4). Then the friction force starts again to increase with new asperity junctions, that are formed as rapidly as the old ones break.

In solution-polymerized polyurethanes, however, the fluorine terminated chain ends were distributed uniformly on the surface and covered most of surface. Even though it has a domain structure, it could not take a role of the adhesive junction due to the uniform distribution of fluorine segments. Consequently, there were no adhesive asperity junctions generated with solution-polymerized polyurethanes, resulting in a smooth sliding friction motion.

4. Conclusions

The surface composition, surface morphology and friction behavior of F-Polyol containing polyurethane elastomers were investigated in terms of the polymerization method and fluorine composition. GPC results showed that the modified polyurethane via melt polymerization had a broader molecular weight distribution compare relative to the solution-polymerized polyurethanes, suggesting the melt polymerization produced inhomogeneous structures. Angle-dependent XPS data showed that fluorine enrichment increased notably at about 1 wt% of F-Polyol and this surface enrichment was more significant in the solution-polymerized polyurethanes. FE-SEM and AFM showed a phase separated morphology and this also suggested that the fluorine depleted regions found in melt-polymerized polyurethanes may cause the lower surface fluorine concentration. The friction coefficient of the F-Polyol containing polyurethanes was significantly lower than the control, and they were inversely proportional to the surface fluorine concentration measured by XPS. Furthermore, a stick-slip type friction behavior was observed exclusively in the melt-polymerized polyurethane. The origin of the stick-slip motion derives from the intrinsic role of PHMC-rich phase as an adhesive junction, in which the hard segments in PHMC-rich phase were located higher than soft-segments, which was also proved by AFM.

Acknowledgements

This study was supported by Omnova Solutions Inc and the National Science Foundation (No. 9975678). The authors are grateful to S. McCartney for FE-SEM and AFM measurements.

References

[1] Woods G. The ICI polyurethane book, 2nd ed. New York: Wiley; 1990.
[2] Noshay A, McGrath JE. Block copolymers; overview and critical survey. New York: Academic Press; 1977.
[3] Schmidt DL, Coburn CE, Dekoven BM, Potter GE, Meyers GF, Fischer DA. Nature 1994;368:39–41.
[4] Yuan Y, Shoichet MS. Macromolecules 2000;33:4926–36.
[5] Ming W, Laven J, Linde R. Macromolecules 2000;33:6886–91.
[6] Sauer BB, McLean RS, Thomas RR. Langmuir 1998;14:3045–51.
[7] Bongiovanni R, Beamson G, Mamo A, Priola A, Recca A, Tonelli C. Polymer 2000;41:409–14.
[8] Jannasch P. Macromolecules 1998;31:1341–7.
[9] Ukpabi PO, Obendrof SK, Puts RD, Sogah DY. J Macromol Sci Pure 1997;A34:1439–56.
[10] Oertel G, editor. Polyurethane handbook. New York: Hanser; 1993.
[11] Zhuang H, Marra KG, Ho T, Chapman TM, Gardella Jr. JA. Macromolecules 1996;29:1660–5.
[12] Ferreri E, Gisvarinl F, Tocelli C, Trombetta T, Zielinski RE. US Patent No. 5,332,798; 22 December 1992.
[13] Cooper SL, Tobolsky AV. J Appl Polym Sci 1966;10:1837–44.
[14] Koberstein JT, Russell TP. Macromolecules 1986;19:714–20.
[15] McLean RS, Sauer BB. Macromolecules 1997;30:8314–7.
[16] Tang YW, Santerre JP, Labow RS, Taylor DG. J Appl Polym Sci 1996;63:1133–45.
[17] Wang LF, Ji Q, Glass TE, Ward TC, McGrath JE, Muggli M, Burns G, Sorathia U. Polymer 2000;41:5083–93.
[18] Ji Q, Kang H, Wang J, Wang S, Glass TE, McGrath JE. Polym Prepr 1999;40:930–1.
[19] Ji Q, Kang H, Wang J, Wang S, Glass TE, McGrath JE. Polym Prepr 2000;41:346–7.
[20] Thomas R, Ji Q, McGrath JE. Polyurethane 2000, ACS Polymer Division Workshop; 25 September 2000.
[21] Wen J, Somorjai G, Lim F, Ward R. Macromolecules 1997;30: 7206–13.
[22] Benoist P, Legeay G. Eur Polym J 1994;30:1283–7.
[23] Hill DJT, Killeen MI, Odonnell JH, Pomery PJ, St John D, Whittaker AK. J Appl Polym Sci 1996;61:1757–66.
[24] Malik AA, Manser GE, Archibald TG. US Patent No. 5,650,483 (to GenCorp, Inc.); 22 July 1997.
[25] Ji Q, McGrath JE. Unpublished results.
[26] Magonov SN, Cleveland J, Elings V, Denley D, Whangbo MH. Surf Sci 1997;389:201–11.
[27] Frommer J. Angew Chem Int Ed Engl 1992;31:1298–328.
[28] Karbach A, Drechsler D. Surf Interf Anal 1999;27:401–9.
[29] Magonov SN, Elings V, Whangbo MH. Surf Sci 1997;375:L385–91.
[30] Berman AD, Ducker WA, Israelachvili JN. Langumir 1996;12: 4559–63.
[31] Ndoni S, Jannasch P, Larsen NB, Almdal K. Langmuir 1999;15: 3859–65.
[32] Baumberger T, Heslot F, Perrin B. Nature 1994;367:544–6.
[33] Yoshizawa H, Chen YL, Israelachvili JN. J Phys Chem 1993;97: 4128–40.
[34] Yoshizawa H, Israelachvili JN. J Phys Chem 1993;97:11300–13.